Investigation of nanodefect properties in optical coatings by coupling measured and simulated laser damage statistics

Laurent Gallais,[a] Jérémie Capoulade, Jean-Yves Natoli, and Mireille Commandré
Institut Fresnel (UMR CNRS 6133), Université Aix Marseille, Ecole Centrale Marseille, Domaine Universitaire de St Jérôme, 13397 Marseille Cedex 20, France

(Received 20 May 2008; accepted 1 July 2008; published online 10 September 2008)

We propose a model to link laser damage initiator properties (such as nature, size distribution, and density) to measured laser damage probabilities in optical materials. The model is based on the calculation of light absorption in nanoabsorbers and subsequent heating, coupled to laser damage statistics, and allows to obtain the laser damage probability as a function of laser fluence. Applications to the case of optical coatings irradiated in the nanosecond regime are presented. Laser damage probability curves are measured in hafnia single layer coatings made under different conditions: electron beam deposition and reactive low voltage ion plating. By studying the influence of the laser irradiation parameters (wavelength and beam size) and coating properties on the simulations, we show with our methodology that initiating defects (hafnium inclusions) can be identified. The implications of this approach for physical understanding and metrology applications are discussed. © *2008 American Institute of Physics*. [DOI: 10.1063/1.2975179]

I. INTRODUCTION

Laser damage of dielectric thin films in the nanosecond regime is mainly initiated by nanometric absorbing defects[1–3] inherent to the manufacturing process. An identification of these defects and understanding of the damage mechanisms could lead to the improvement of the manufacturing process. However, in the case of high quality coatings, the defects are not detectable by conventional techniques before any macroscopic damage occurs. Hence their nondestructive detection is still an issue for the community.

Since laser damage is linked to defects, damage initiation is localized and probabilistic. A useful method to obtain information on the damaging defects is to study the laser damage statistics: for instance, plotting the laser damage probability as a function of fluence. Simple models have been developed in order to relate the defect properties (such as the density) and experimental parameters (such as the spot size) to the damage statistics.[4–9] This is done by assuming that the probability of damage is the probability that a defect with a certain intrinsic threshold is present in the irradiated area where the fluence is higher than the defect threshold. With the defects being unknown, different hypotheses were made about the defect ensembles and their threshold distribution (Dirac, power law, Gaussian law, etc.). Recently, thermal models coupled to statistics were proposed, based on damage initiation by heating of size-distributed inclusions[10,11] or cluster of defects[12] to a critical temperature. These approaches have proved to be successful for the qualitative interpretation of experimental data, such as temporal and wavelength dependence of the damage probability, and conditioning effects in the case of potassium dihydrogen phosphate (KDP) crystals.

In the case of optical coatings, a first attempt to extract the physical properties of defects from laser damage measurements was presented in Ref. 13: it was shown by comparing laser damage statistics and heat transfer in absorbing inclusions that the complex refractive index and the size of precursors could be estimated. In this paper we go further in these investigations using the nanoabsorber model to identify (or eliminate) potential defects in optical coatings, responsible for initiation of damage. The spot size dependence is considered up to the case of very small beam sizes (few micrometers diameters). Furthermore the cases of surfaces, bulk materials, and thin films are addressed.

In the first part Section II, we detail the model developed for this study. It is based on the calculation of absorption of spherical absorbers, then solving of the heat equation for nanosecond pulsed laser irradiation and calculation of the laser damage probability taking into account the defect size distribution and density. In Section III, dedicated to experiments, the samples under study (hafnia monolayers) and their fabrication processes are described. The experimental setup used to measure laser damage probability curves with high accuracy is detailed. The results of the laser damage tests made in one on one mode with different spot sizes and wavelengths are given. These results are analyzed and discussed in Section IV: the model is applied to fit the results in order to identify potential initiating defects.

II. MODEL

The aim of the model is to simulate laser damage probability curves by calculating the fluence necessary to initiate damage as a function of the defect properties. Nevertheless we want to keep the model as simple as possible and reasonable simplifications can be made for this. Below we detail the different assumptions that have been made, and discuss their validity and limitations.

- The precursors are assumed to be spherical. Nonspherical shapes (rods and plates) can also be

[a]Electronic mail: laurent.gallais@fresnel.fr. URL: www.fresnel.fr.

considered,[14] but are more adapted to the case of crystals where planar defects, for instance, can be involved.

- Precursors have a size distribution and a homogeneous density. The size distribution is of course unknown. We consider that the size distribution follows a power law, as commonly observed for clusters embedded in solid materials.[15] This is detailed in Sec. II C. Another approach[12] is to consider a random distribution of identical defects (same size) that can aggregate and thermally cooperate to create damage. In fact, this approach is very similar since the critical element is the cluster size and the distribution in size.
- All parameters are independent of the temperature. Particularly the thermal parameters of the inclusion certainly vary with temperature, but it has been shown that large variations in the thermal properties of the defect only weakly affect temperature predictions by the inclusion-dominated model of laser-induced damage.[16]
- Because of the small size of considered precursors in comparison with the thermal diffusion length, the energy deposition is considered uniform throughout the precursor.
- We assume that damage is reached when the temperature of the surrounding matrix exceeds a critical value (for instance, the melting point). This is an arbitrary criterion, but it is based on the fact that above a critical temperature a thermal runaway process takes place,[17] leading to damage. We can note that the maximum temperatures reached in our approach are relatively low compared to the one measured in the real process which can reach 10 000 K.[18]
- Only losses by heat conduction are considered. This is certainly a limitation since it has been shown that energy transfer by radiation has to be taken into account in the laser damage mechanism.[19]

A. Optical and thermal properties of inclusions

When dealing with nanometric to micrometric defects, it is usual to consider in calculation the bulk material properties. However, for small particles the dielectric function "ϵ" depends on the particle size and differs from the bulk values because of the increasing importance of the surfaces compared to the volume, the change of the atomic structure, and the inhomogeneities of the electron density. We want to use the Mie theory to evaluate the absorption of a defect; thus we need of course to use the appropriate dielectric function. Consequently the problem is to first find the size limit for the validity of bulk value and second to find a model that describes ϵ as a function of the size.

In the case of metals, if we consider the Drude model, the complex dielectric function can be expressed as

$$\epsilon(\omega) = 1 - \frac{\omega_p^2}{\omega(\omega + i\Gamma)}, \tag{1}$$

where ω_p is the plasma pulsation and Γ is a damping term. This coefficient is related to the electron mean free path l by $\Gamma = v_F/l$, where v_F is the Fermi velocity. The mean free path in the case of the bulk material (denoted as l_∞) is linked to interactions with phonons, electrons, impurities, lattice defects, etc. However, in the case of a small particle the particle size can become comparable or smaller than l_∞, and interactions of electrons with the surface have to be taken into account. This leads to an effective mean free path smaller than l_∞ which is referred to the *free path effect* for small clusters. Then a reasonable value of the cluster size (radius R) for the application of the bulk dielectric function is $2R \geq l_\infty$. The order of magnitude of the mean free path in metals is of 10 nm to few tens of nanometers depending on the material.[15] In the case of clusters of few nanometers, the dielectric function is therefore different from the bulk one.

A number of different approaches have been developed for the calculation of ϵ as a function of the cluster size.[15] These different approaches lead to the conclusion that a contribution linked to the cluster size has to be added to the damping term Γ in the Drude model:

$$\Gamma(R) = \Gamma_\infty + \Delta\Gamma(R), \tag{2}$$

and that this contribution is proportional to $1/R$:

$$\Delta\Gamma(R) = A\frac{v_F}{R}. \tag{3}$$

Applying formulas (1)–(3) we can take into account the defect size in the inclusion-dominated model of laser damage. However, we will see in Section II C that clusters of few nanometers cannot initiate damage under our working conditions: their absorption cross section is so weak that fluences of several orders of magnitude higher than the measured threshold are needed to reach the melting point. As a consequence we will use the bulk properties of metals for estimating the inclusion absorption and finally the temperature elevation under irradiation.

Similar remarks can be made on the thermal conductivity since this parameter depends on the electronic mean free path. The bulk thermal properties of the metal will then also be used for our calculations.

In the case of dielectric particles, we will see that relatively large particles have to be involved to initiate damage; thus the bulk values can be used in this case too.

B. Absorption

We consider a dielectric or metallic absorbing particle (complex refractive index: $\tilde{n} = n + ik$) embedded in a transparent material without absorption.

The absorbed power by a spherical absorbing particle is

$$Q = \sigma I, \tag{4}$$

where σ is the absorption cross section and I is the intensity in W/cm^2. The absorption cross section is calculated with the Mie theory.[20]

We plotted in Fig. 1 the absorption cross section of a hafnium spherical particle in a hafnia matrix. This kind of metallic defect can be found in hafnia coatings so we chose to use it throughout this section as an illustration of the model.

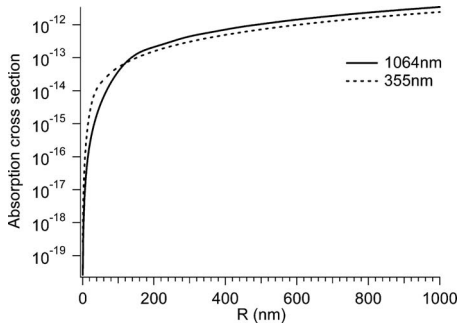

FIG. 1. Absorption cross section calculated with Mie theory for a hafnium inclusion in a hafnia matrix.

C. Critical fluence

Damage is assumed to take place when the temperature of the inclusion reaches a critical value T_c. The fluence necessary to reach this value is called the critical fluence F_c.

To calculate the temperature we solve the heat equation under the assumptions detailed before. For this calculation we do not use the classical approximation of Hopper and Uhlmann[21] (high thermal conductivity for the defect) since the solution fails for dielectric impurities,[22] but we numerically calculate the solution in order to take into account either metallic or dielectric defects that can be found in thin films. We consider a Gaussian temporal profile for the irradiation to be closer to the experimental conditions. Indeed, it has been experimentally shown by Carr *et al.* that the temporal pulse shape has an effect on laser damage.[23] The details of the thermal part of the model are exposed in Ref. 13.

By calculating the heating of the inclusion as a function of the fluence, we find the critical fluence required to reach T_c. Furthermore by iterating this calculation for different absorber radii, F_c can be plotted as a function of the inclusion size. This has been done for illustration in Fig. 2 in the case of the hafnium inclusions in a hafnia matrix, with T_c chosen as the melting temperature of hafnia.

In the case of very small absorbers, the absorptivity decreases dramatically as the size decreases (Fig. 1). Therefore the value of the fluence necessary to damage rises (Fig. 2). On the contrary, for large particles, the pulse is too short in time to heat them since they contain too much matter. As a consequence there is an inclusion size most susceptible to create damage, and this size depends on the pulse duration, as first pointed out by Hopper and Uhlmann.[21] In the case of hafnium inclusions in hafnia (Fig. 2) the critical radius is about 150 nm at 1064 nm and 100 nm at 355 nm. However, if these inclusions are the most susceptible to create damage, they are not the damage initiators found in high quality coatings since damage initiates on areas free from any visible defects. Indeed, in the case of particles of few 100 nm in films of the same few 100 nm thickness, the defects should be detectable by classical optical techniques. As a consequence, only the left part of the critical fluence curves is of interest for our application.

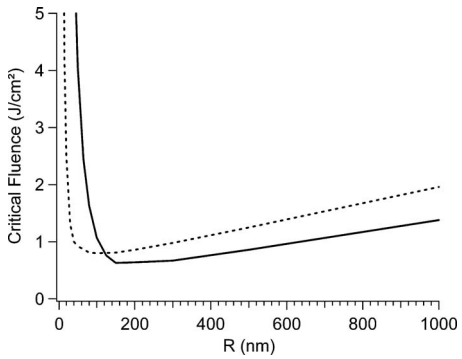

FIG. 2. Critical fluence calculated for a hafnium inclusion in a hafnia matrix. Irradiation is at 1064 or 355 nm with a pulse duration of 12 ns at $1/e$ (Gaussian temporal shape).

D. Laser damage probability

The standard measurement in laser damage experiments is to plot the damage probability as a function of the fluence.[24] If we assume that damage occurs if a defect is irradiated with a fluence higher than F_c, this damage probability can be theoretically calculated and compared to experiments.

However, F_c depends on the precursor size, and the size distribution of defects is unknown. Without knowledge of this distribution we chose to consider a power law distribution since this type of variation is typically found for clusters.[15] These distributions are also often observed in natural processes such as optics contamination.[14] The distribution of defects in our model is then assumed to follow the law:

$$\rho(R) = A/R^{\alpha}, \tag{5}$$

where A is a constant that will be explained later. In fact, we expect that there are much more small precursors than large ones, and the coefficient "α" will be a fit parameter of the model. In addition only a range of size is of interest since very small/large precursors are not susceptible to damage as seen before. As a consequence, we insert lower and upper limits for calculation convenience ($R_{\min}$ and $R_{\max}$). Then we obtain an expression for A:

$$A = (1-\alpha)d_0/(R_{\max}^{1-\alpha} - R_{\min}^{1-\alpha}), \tag{6}$$

with d_0 the total density of defects per unit of volume or surface (volume or surface defects can be considered). This parameter is also chosen as a fit parameter of the model.

The defect population can be described by the ensemble function $g(F_c)$, which gives the number of defects per unit of volume that damage at fluence (or threshold) between F_c and $F_c + dF_c$. The relationship between $g(F_c)$ and the defect density d is

$$\int_0^{\infty} g(F_c)dF_c = d. \tag{7}$$

With the knowledge of the critical fluence (damaging fluence as a function of size) and the defect size distribution (density as a function of size) one can obtain the function $g(F_c)$ (density of damaging defects as a function of fluence). This calculation is done numerically in our case. An example is shown in Fig. 3 for the case of hafnium inclusions in hafnia, with an arbitrary value for α and d.

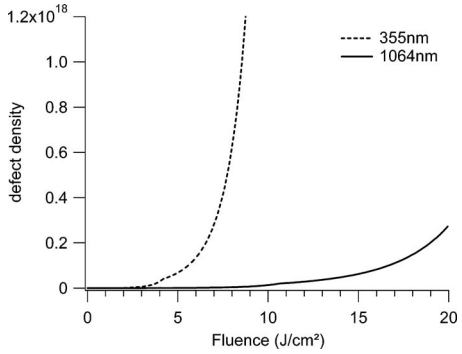

FIG. 3. $g(F_c)$ function (defect repartition as a function of their damaging fluence F_C) calculated for a hafnium inclusion in a hafnia matrix. Irradiation is at 1064 or 355 nm with a pulse duration of 12 ns at $1/e$ (Gaussian temporal shape). The parameter α was set to 3.

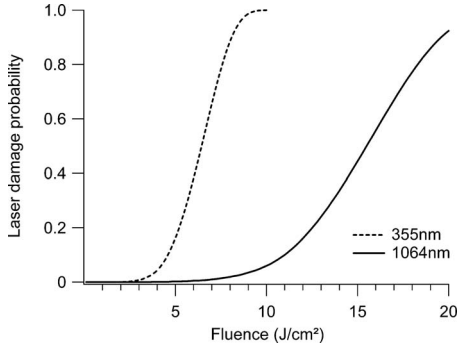

FIG. 4. Laser damage probability curves calculated for a hafnia film (mechanical thickness of 100 nm) containing hafnium inclusions. Irradiation is at 1064 or 355 nm with a pulse duration of 12 ns at $1/e$.

The probability of damage $P(F)$ is the probability of the presence of a defect that receives more energy density than its critical fluence. This probability can classically be expressed as

$$P(F) = 1 - \exp[-N(F)], \tag{8}$$

where $N(F)$ is the number of defects under the laser spot that can induced damage at the fluence F.

- In the case of surface precursors, the number of defects $N(F)$ located under the laser spot of fluence F and whose threshold is lower than F is

$$N(F) = \int_0^F g(F_C) S_{F_C}(F) dF_C, \tag{9}$$

with $S_{F_C}(F)$ the part of the spot size where the fluence F is greater than the precursor critical fluence F_C. If a Gaussian beam is considered, $S_{F_C}(F)$ is

$$S_{F_C}(F) = \frac{\pi\omega^2}{2} \ln\left(\frac{F}{F_C}\right), \tag{10}$$

with ω the beam waist radius.

- In the case of bulk precursors the number of defects $N(F)$, localized in the volume under irradiation and whose threshold is lower than F, is

$$N(F) = \int_0^F g(F_C) V_{F_C}(F) dF_C, \tag{11}$$

with $V_{F_C}(F)$ the volume where the fluence F is greater than the precursor critical fluence F_C. If a Gaussian beam is considered, $V_{F_C}(F)$ is

$$V_{F_C}(F) = \frac{4}{3}\omega_0^2 Z_R \left(\frac{\sqrt[3]{\frac{F}{F_C} - 1}}{6} + \sqrt{\frac{F}{F_C} - 1} - \arctan\left(\sqrt{\frac{F}{F_C} - 1}\right)\right), \tag{12}$$

with Z_R the Rayleigh length and ω_0 the beam waist.

- In the case of thin films we have to take into account the electric field repartition, particularly if we deal with a multilayer system. The number of defects $N(F)$ can then be expressed as

$$N(F) = \int_0^F g(F_C) V^e_{F_C}(F) dF_C, \tag{13}$$

with $V^e_{F_C}$ an efficient volume where the fluence F is greater than the precursor critical fluence F_C:

$$V^e_{F_C} = \frac{\pi}{2} \int_0^e \omega^2(z) \ln\left(\frac{F(z)}{F_C} \frac{\omega_0}{\omega^2(z)}\right) dz, \tag{14}$$

with e the mono- or multilayer total thickness and z the orthogonal direction to the films. $F(z)$ (or energy density repartition in the films) can be easily obtained with classical electric field calculations in thin films.[25]

With this model we have the ability to describe laser damage in surface, bulk, or thin films as a function of three physical characteristics: the defect composition, the size distribution of defects, and their density in the material.

We plot for illustration (Fig. 4) the theoretical laser damage probability curves calculated in the case of hafnia thin films containing hafnium inclusions with distribution of size. A typical S-curve is obtained, as observed in experiments.

III. EXPERIMENTS

A. Samples

The samples under study are HfO_2 single layer coatings. This material has been chosen for our study because it is one of the most important high index materials for the production of optical coatings for UV to IR high power laser applications. For damage resistance, it is known to be the limiting material in silica/hafnia multilayer coatings.[26]

A Balzers BAP 800 reactive ion plating (IP) system was used to deposit the coatings from hafnium starting material. A run of samples were made through a standard electron beam deposition (EBD) process and another run using the argon ion plasma assistance. Except for the assistance, the deposition parameters were the same for both series of samples (see Table I). These parameters correspond to the optimized process developed at the Fresnel Institute for this material.[27] The substrates were 1 in. diameter fused silica

TABLE I. Sample description.

Reference	Optical thickness	Deposition parameters
EBD 2H@1064	λ/2 at 1064 nm	Deposition technique: EBD Source material: Hf 99.5% (Umicore granulate) Liner: carbon; voltage: 10 kV
EBD 2H@355	λ/2 at 355 nm	Base pressure: 3×10^{-7} mbar Partial pressure (O_2): 5×10^{-4} mbar Deposition rate: 0.9 nm/s; substrate temperature (250 °C)
IP 2H@1064	λ/2 at 1064 nm	Deposition technique: RLVIP Source material: Hf 99.5% (Umicore granulate) Liner: carbon; voltage: 10 kV
IP 2H@355	λ/2 at 355 nm	Base pressure: 3×10^{-7} mbar Partial pressure ($Ar+O_2$)mbar: 6×10^{-4} Deposition rate: 0.2 nm/s; substrate temperature (250 °C) Assistance parameters: plasma source (55 A, 66 V)

substrates (Corning 7980) polished for high power applications. All the substrates were coming from the same batch and have been polished at the same time.

Since we want to study the influence of the wavelength on the laser damage behavior, samples of different thickness were made with the two techniques: half wave at 1064 nm (made for testing at 1064 nm) and half wave at 355 nm (made for testing at 355 nm). In this way the standing electric field in the coating is the same at the two wavelengths and the results can be easily compared. The sample denominations used in this paper are referenced in Table I.

B. Laser damage probability measurements

Laser damage probability curves were measured at 1064 and 355 nm using an injected Nd:YAG laser (Quantel YG 980) with a pulse duration of 12 ns (effective pulse duration[24] at $1/e$). The laser beam was linearly polarized and focused at normal incidence at the front face of the coated samples. Different spot diameters were used for the tests: 44 and 320 μm at 1064 nm and 3 μm at 355 nm. The damage detection was done by comparing the area before and after irradiation with an imaging system (magnification ×200) and an image processing software. The damage criterion is then any visible modification detected with this system. The damage test procedure one on one mode was applied, with a large number of points to obtain a reliable measurement: each curve $P(F)$ is plotted with 1000 data points that involve 20 different fluencies and 50 tested sites at each fluence in the case of the 3 and 44 μm beam size tests and 400 data points (20 fluences ×20 sites) in the case of the 320 μm beam size tests. The error bars for the probability measurements are calculated using the procedure described in Ref. 28. The error bars in this paper correspond to a confidence level of 95%. The damage probability curves obtained under these conditions on the two different samples [EBD and reactive low voltage ion plating (RLVIP)] are reported in Figs. 5 and 6.

Uncoated samples have also been tested. In comparison to the coatings, the front surface Laser Induced Damage Threshold (LIDT) of the uncoated substrate samples was 80 J/cm^2 at 1064 nm and 20 J/cm^2 at 355 nm in the same test conditions.

The damage morphology observed near threshold fluences consists of one or several micronic pits localized under the irradiated area. Several images of the typical morphologies observed for both deposition technologies are given in Fig. 7.

The morphology clearly evidences an initiation process by very small defects. However, the size of the pits cannot be linked directly to the precursor size (except by giving a

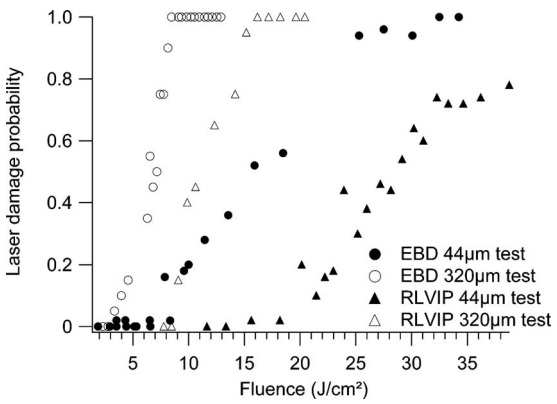

FIG. 5. Results of the laser damage tests made at 1064 nm. Test conditions: one on one mode, 12 ns, 44 and 320 μm spot diameters (at $1/e^2$).

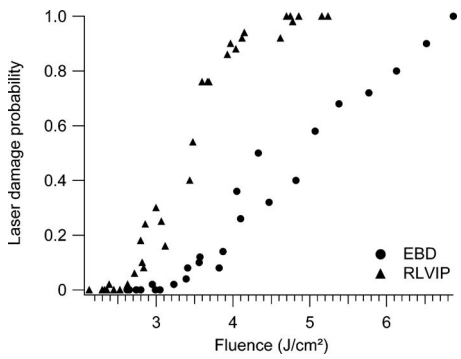

FIG. 6. Results of the laser damage tests made at 355 nm. Test conditions: one on one mode, 12 ns, 3 μm spot diameter (at $1/e^2$).

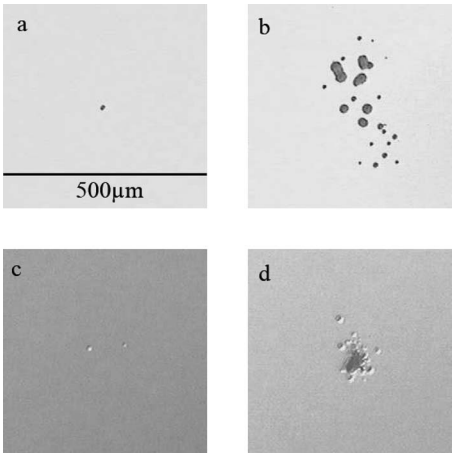

FIG. 7. Laser damage morphologies observed on the samples after irradiation at 1064 nm/12 ns with a beam diameter of 320 μm. (a) RLVIP sample irradiated near the LIDT. (b) RLVIP sample irradiated at high fluence, compared to the LIDT, to emphasize the pits. (c) EBD sample irradiated near the LIDT. (d) EBD sample irradiated at high fluence.

maximum value). Indeed, the pit diameter is linked in a complex way to the size of the laser damage precursor and also depends strongly on the thermal and mechanical properties, residual stresses, and adhesion of the film. For instance, Papernov and Schmid[29] stated that the pit diameter in silica thin films can reach ten times the initiator diameter.

IV. RESULTS AND DISCUSSION

The laser damage initiation on the hafnia coatings under test is initiated by subwavelength precursor defects. In order to identify the damaging precursor defects, we have applied the model described in Sec. II. With the nature of the precursors being unknown, our approach has been to try different potential candidates and compare the theoretical results to the measurements. We have considered two different kinds of absorbing defects that are potential initiators in HfO_2.[19]

- Metallic Hf nanoclusters, with bulk-metal optical and thermal parameters (parameters given in Table II).
- Nonstoichiometric HfO_2 defects, with thin-film real index and thermal parameters but with an imaginary index to account for absorption (parameters given in Table II).

A. Spot size dependence

We first consider the results obtained on the RLVIP sample tested at 1064 nm. For this sample a spot size dependence is observed as expected from the theory: the measured low threshold is 8 J/cm^2 in the case of the 320 μm spot size and 15 J/cm^2 in the case of the 44 μm spot size. For comparison, we have calculated the critical fluence curves obtained for hafnium defects or nonstoichiometric HfO_2 defects embedded in a bulk hafnia matrix. The results are given in Fig. 8.

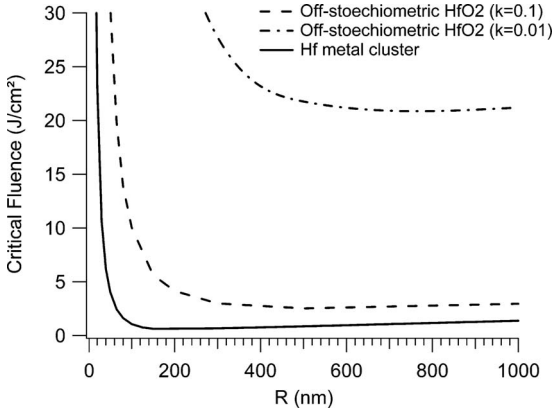

FIG. 8. Critical fluence calculated for different inclusions (hafnium metal or off-stoichiometric absorbing HfO_2 defects) in a hafnia matrix. Irradiation is at 1064 nm with a pulse duration of 12 ns at $1/e$ (Gaussian temporal shape).

Considering these calculations and the thresholds measured on the samples, it appears that dielectric defects cannot be precursors of damage under our assumptions. Indeed, with an extinction coefficient of approximately 10^{-2}, defects cannot induce damage at the level of the measured fluence: 8 J/cm^2. If the extinction coefficient was larger ($\approx 10^{-1}$), dielectric defects could induce damage at 8 J/cm^2, but their size needs to be more than 100 nm, which is almost the layer thickness. These large defects would be visible under the microscope. However, the comparison of Fig. 8 with the measured damage threshold shows that hafnium defects of few tens of nanometers are potential initiators. We now apply our model with hafnium defects to fit the experimental data points in order to check the validity of this assumption. A very good agreement was obtained between the data and the theory, as shown in Fig. 9, when considering a defect size distribution between 5 and 55 nm (and $\alpha=4$). The interesting point is that the model can describe the observed spot size dependence since with the same parameters the data obtained with the two different spot sizes can be fitted.

B. Influence of the deposition technique

In the case of the electron beam deposited layers, the same deposition plant was used, the same materials, as well

TABLE II. Material thermal and optical parameters.

Material	Real index n	Imaginary index k	Conductivity	Diffusivity
Bulk HfO_2 [a]	2 at 1064 nm 2 at 355 nm	0 at 1064 nm 0 at 355 nm	1.67 W/m K	6.8×10^{-7} m^2/s
Hf inclusion[a]	4.08 at 1064 nm 1.71 at 355 nm	3.1 at 1064 nm 2.58 at 355 nm	18.4 W/m K	9.9×10^{-6} m^2/s
Nonstoichiometric HfO_2 inclusions	2 at 1064 nm 2 at 355 nm	0.01–1 at 1064 nm 0.01–1 at 355 nm	1.67 W/m K	6.8×10^{-7} m^2/s

[a]Reference 30.

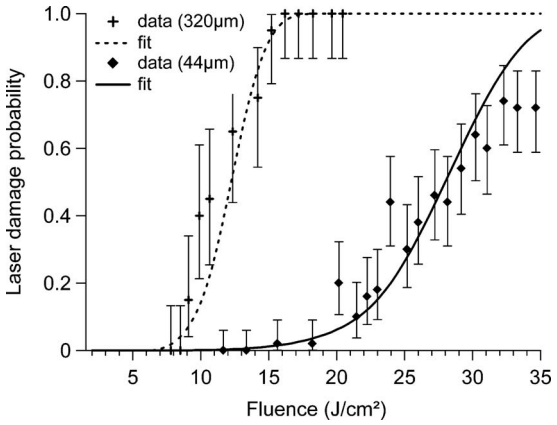

FIG. 9. Laser damage probability measured (at 1064 nm/12 ns) for a hafnia film made by RLVIP (half wave at 1064 nm). The calculated curves are plotted for the same values of fit parameters for both beam sizes.

as the same parameters, except for the assistance. Thus one would expect similar defects to be present in both types of films. However, lower thresholds were measured for the EBD layers at 1064 nm, as shown in Fig. 5. To explain these results, one should consider that the mechanical and thermal properties of these coatings are different from the dense ones obtained with plasma assistance. Indeed, EBD films are known to exhibit a porous structure.[31] This is confirmed on our samples by the refractive index deduced from spectrophotometry measurements. For the EBD coatings we obtain $n=1.92$ at 1064 nm, compared to the IP coatings: $n=2.21$ at 1064 nm. This last refractive index is very close to the bulk value reported for hafnia.[32] Heat transport in EBD films is influenced by the columnar structure of the films, and the thermal conductivity of the coated material may be smaller than that of the bulk. From the few studies in literature devoted to the thermal properties of optical thin films,[33–38] it appears that the thermal properties of EBD coatings, particularly the thermal conductivity, are strongly dependent on the deposition process and can differ by several orders of magnitude from those of bulk materials. The thermal conductivity of the matrix is of critical importance for the laser damage threshold in the case of an absorbing inclusion driven mechanism.[22] In order to study the influence of the thermal conductivity of the host material on the damage threshold, we plotted in Fig. 10 the critical fluence calculated for a

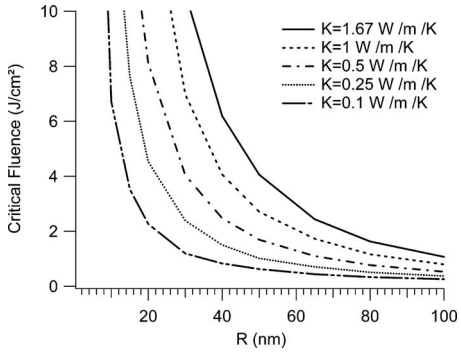

FIG. 10. Critical fluence calculated for a hafnium inclusion in a hafnia matrix with different conductivities. Irradiation is at 1064 nm with a pulse duration of 12 ns at $1/e$ (Gaussian temporal shape)

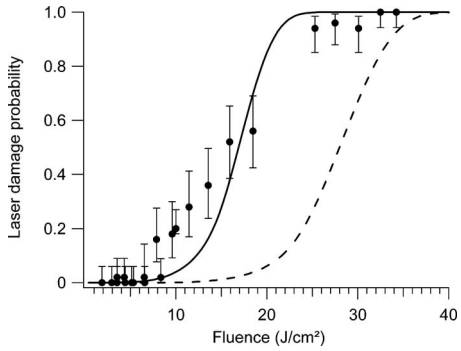

FIG. 11. Laser damage probability measured with a beam spot size of 44 μm (at 1064 nm/12 ns) for a hafnia film made by EBD (half wave at 1064 nm). The fits of the experimental data are made with the same parameters found on the films obtained by IP (dotted line) and with a thermal conductivity of 0.68 W/m K (plain line).

hafnium inclusion in a hafnia matrix with different thermal conductivities.

Based on these simulations we tried to fit the laser damage probabilities obtained on the EBD samples using the same defect parameters found on the IP samples but adjusting the thermal conductivity of the host material. We found that with a thermal conductivity of 0.7 W/m K (to be compared to the bulk one: 1.67 W/m K) a reasonable agreement was obtained for the small beam size test results (even if the shape of the curve differs) and a very good agreement was obtained for the large beam size test results (Figs. 11 and 12). Hence, even if the defect distribution may be slightly different, the model describes damage probability curves on dense and porous coatings for two different laser beam sizes on each coating.

C. Wavelength dependence

The other samples, half wave at 355 nm, made with the same techniques and in the same conditions, were laser damage tested at 355 nm, 12 ns, with a spot size of 3 μm, as shown in Fig. 6. Since these coatings were made in the same conditions as the 1064 nm samples, a simple assumption would be that the same defects are embedded in both kinds of samples. Then the theoretical laser damage probability curve at 355 nm may be obtained by using the parameters

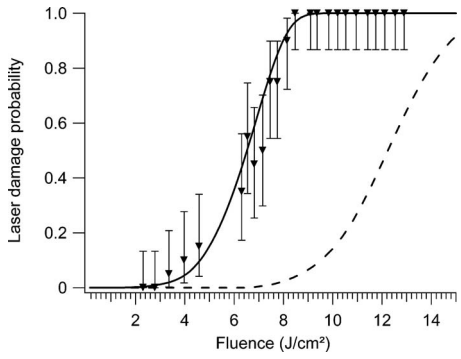

FIG. 12. Laser damage probability measured with a beam spot size of 320 μm (at 1064 nm/12 ns) for a hafnia film made by EBD (half wave at 1064 nm). The fits of the experimental data are made with the same parameters used for the films obtained by IP (dotted line) and with a thermal conductivity of 0.68 W/m K (plain line).

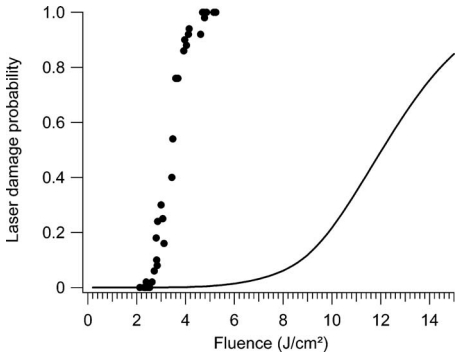

FIG. 13. Laser damage probability curve measured at 355 nm,12 ns, with a spot size of 3 μm for a hafnia film made by RLVIP (half wave at 355 nm). The plain line is the theoretical laser damage probability curve obtained by applying the parameters found at 1064 nm to the 355 nm case.

found previously (defect distribution) and by calculating the critical fluence at 355 nm for hafnium. The result of this calculation is plotted in Fig. 13.

Obviously, a large discrepancy is found between theory and experiment. The measured laser damage threshold is found to be lower than the one expected with our simple assumptions. Since it appears difficult to imagine different defects more absorbing than metallic clusters, the explanation is perhaps to be found in the laser damage mechanism and the theoretical damage criterion that we apply. Indeed, it has been shown experimentally in the case of UV irradiation that the material around a damage initiator defect is modified during the laser pulse.[39,40] When a nanoabsorber is strongly heated, energy is transferred to the surrounding matrix (by conduction and radiation). Subsequently, the matrix is modified and can be converted into an absorbing material. This additional absorption around the defect is perhaps critical in the case of UV irradiation compared to IR irradiation (far from the absorption band of HfO_2) and could explain these discrepancies between theory and experiment. This is clearly a limitation of our approach, and refined models have to be used in this case.

V. CONCLUSION

A model has been developed in order to relate the material properties of initiating defects to the laser damage probability as a function of fluence. Different assumptions that have been clearly detailed have been made in order to keep the approach simple.

The model has been applied to the study of hafnia thin films made with different deposition technologies. Different laser damage tests were conducted on the samples. At 1064 nm, the results show a good agreement between measurements and theoretical predictions and demonstrate the validity of the approach. In the studied samples, hafnium clusters with diameters order of magnitude of 10 nm have been identified as damaging defects. A very good agreement with the spatial scaling law has been observed. Thus an application of this study is to obtain functional threshold of optical components.

Of course the results must be taken with caution since different assumptions have been made for the calculations, but it is interesting to point out that all the results obtained (laser damage spot size and material property dependence) have been explained with the same kind of defects having a given density and size distribution. The interest of this approach is of course not to identify with certainty the defects but to highlight potential candidates.

One perspective is now to extend this model to the case of repetitive shots since it is known that successive shots can increase (conditioning effect) or decrease (fatigue effect) the LIDT depending on the material. For this purpose, modification of the defect properties under successive irradiations will be taken into account.

ACKNOWLEDGMENTS

We thank the RCMO team of the Institut Fresnel for manufacturing the samples. Funding of this work by the European Union (Grant Nos. FEDER 2646 and FSE 2003.21.02.0037), the region PACA, and the Conseil General des BDR is gratefully acknowledged.

APPENDIX: PARAMETERS USED FOR CALCULATION

The parameters used in the calculations are listed in Table II.

[1] D. Milam, R. A. Bradbury, and M. Bass, Appl. Phys. Lett. **23**, 654 (1973).
[2] M. R. Kozlowski and R. Chow, in *Laser-Induced Damage in Optical Materials: 1993*, edited by H. E. Bennet, A. H. Guenther, M. R. Kozlowski, B. E. Newnam, and M. J. Soileau (SPIE, Bellingham, WA, 1994), Vol. 2114, p. 640.
[3] J. Dijon, T. Poiroux, and C. Desrumaux, in *Laser-Induced Damage in Optical Materials: 1996*, edited by H. E. Bennett, A. H. Guenther, M. R. Kozlowski, B. E. Newnam, and M. J. Soileau (SPIE, Bellingham, WA, 1997), Vol. 2966, p. 315.
[4] R. Picard, D. Milam, and R. Bradbury, Appl. Opt. **16**, 1563 (1977).
[5] J. O. Porteus and S. C. Seitel, Appl. Opt. **23**, 3796 (1984).
[6] R. M. O'Connell, Appl. Opt. **31**, 4143 (1992).
[7] J. Y. Natoli, L. Gallais, H. Akhouayri, and C. Amra, Appl. Opt. **41**, 3156 (2002).
[8] H. Krol, L. Gallais, C. Grèzes-Besset, J. Y. Natoli, and M. Commandré, Opt. Commun. **256**, 184 (2005).
[9] Z. Xia, Z. Fan, and J. Shao, Opt. Commun. **265**, 620 (2006).
[10] M. D. Feit and A. M. Rubenchik, in *Laser-Induced Damage in Optical Materials: 2003*, edited by G. J. Exarhos, A. H. Guenther, N. Kaiser, K. L. Lewis, M. J. Soileau, and C. J. Stolz (SPIE, Bellingham, WA, 2004), Vol. 5250, p. 74.
[11] A. Dyan, F. Enguehard, H. Piombini, S. Lallich, and G. Duchateau, J. Opt. Soc. Am. B **25**, 1087 (2008).
[12] G. Duchateau and A. Dyan, Opt. Express **15**, 4557 (2007).
[13] L. Gallais, P. Voarino, and C. Amra, J. Opt. Soc. Am. B **41**, 4023 (2003).
[14] J. B. Trenholme, M. D. Feit, and A. M. Rubenchik, *Laser-Induced Damage in Optical Materials–2005*, edited by G. J. Exarhos, A. H. Guenther, K. L. Lewis, D. Ristau, M. J. Soileau, and C. J. Stolz (SPIE, Bellingham, WA, 2005), Vol. 5991, p. 59910X.
[15] U. Kreibig and M. Vollmer, *Optical Properties of Metal Clusters* (Springer, New York, 1995).
[16] M. Z. Fuka, J. K. McIver, and A. H. Guenther, *Laser-Induced Damage in Optical Materials–1989*, edited by H. E. Bennett, L. L. Chase, A. H. Guenther, B. E. Newnam, and M. J. Soileau (SPIE, Bellingham, WA, 1990), Vol. 1438, p. 576.
[17] M. F. Koldunov, A. A. Manenkov, and I. L. Pokotilo, Sov. J. Quantum Electron. **20**, 456 (1990).
[18] C. W. Carr, H. R. Radousky, A. M. Rubenchik, M. D. Feit, and S. G. Demos, Phys. Rev. Lett. **92**, 087401 (2004).
[19] S. Papernov and A. W. Schmid, J. Appl. Phys. **82**, 5422 (1997).
[20] We used the S1 code (available at http://atol.ucsd.edu/ pflatau/) described in P. W. Barber and S. C. Hill, *Light Scattering by Particles: Computational Methods* (World Scientific, Singapore, 1990).
[21] R. W. Hopper and D. P. Uhlmann, J. Appl. Phys. **41**, 4023 (1970).

[22]T. W. Walker, A. H. Guenther, and P. Nielsen, IEEE J. Quantum Electron. **17**, 2053 (1981).
[23]C. W. Carr, J. B. Trenholme, and M. L. Spaeth, Appl. Phys. Lett. **90**, 041110 (2007).
[24]ISO Standard 11254-1, 2000.
[25]H. A. MacLeod, *Thin Film Optical Filter*, 3rd ed. (Institute of Physics Publishing, Bristol and Philadelphia, 2001).
[26]C. J. Stolz and F. Génin, *Optical Interference Coatings*, edited by N. Kaiser and H. Pulker (Springer, New York, 2003).
[27]L. Gallais, J. Capoulade, J. Y. Natoli, M. Commandé, M. Cathelinaud, C. Koc, and M. Lequime, Appl. Opt. **47**, C107 (2008).
[28]A. Hildenbrand, F. Wagner, H. Akhouayri, J. Y. Natoli, and M. Commandé, Opt. Eng. **47**, 083603 (2008).
[29]S. Papernov and A. W. Schmid, J. Appl. Phys. **97**, 114906 (2005).
[30]*CRC Handbook of Chemistry and Physics*, 87th ed., edited by D. R. Lide (Taylor and Francis, Boca Raton, FL, 2007).
[31]J. Yao, Z. Fan, Y. Jin, Y. Zhao, H. He, and J. Shao, J. Appl. Phys. **102**, 063105 (2007).
[32]D. L. Wood, K. Nassau, T. Y. Kometai, and D. L. Nash, Appl. Opt. **21**, 604 (1990).
[33]R. T. Swimm, Appl. Phys. Lett. **42**, 955 (1983).
[34]D. Ristau and J. Ebert, Appl. Opt. **25**, 4571 (1986).
[35]M. Rohde, Thin Solid Films **238**, 199 (1994).
[36]E. Welsch and D. Ristau, Appl. Opt. **34**, 7239 (1995).
[37]A. Ocariz, A. Sanchez-Lavega, A. Salazar, D. Fournier, and A. C. Boccara, J. Appl. Phys. **80**, 2968 (1996).
[38]Z. L. Wu, M. Thomsen, P. K. Kuo, Y. Lu, C. J. Stolz, and M. Kozolowski, Opt. Eng. **36**, 251 (1997).
[39]M. A. Stevens-Kalceff, A. Stesmans, and J. Wong, Appl. Phys. Lett. **80**, 758 (2002).
[40]F. Bonneau, P. Combis, J. L. Rullier, M. Commandre, A. During, J. Y. Natoli, M. J. Pellin, M. R. Savina, E. Cottancin, and M. Pellarin, Appl. Phys. Lett. **83**, 3855 (2003).